

Automated Vegetative Stage Phenotyping Analysis of Maize Plants using Visible Light Images

Sruti Das Choudhury^{*}
Department of Computer
Science and Engineering
University of Nebraska-Lincoln
Lincoln, NE, USA
S.D.Choudhury@unl.edu

Vincent Stoerger
Plant Phenotyping Facilities
Manager
University of Nebraska-Lincoln
Lincoln, NE, USA
vstoerger2@unl.edu

Ashok Samal
Department of Computer
Science and Engineering
University of Nebraska-Lincoln
Lincoln, NE, USA
samal@cse.unl.edu

James C. Schnable
Department of Agronomy and
Horticulture
University of Nebraska-Lincoln
Lincoln, NE, USA
schnable@unl.edu

Zhikai Liang
Department of Agronomy and
Horticulture
University of Nebraska-Lincoln
Lincoln, NE, USA
zliang@huskers.unl.edu

Jin-Gang Yu
Department of Computer
Science and Engineering
University of Nebraska-Lincoln
Lincoln, NE, USA
jingangyu@unl.edu

ABSTRACT

Extracting meaningful numerical phenotypes from plant images remains a substantial bottleneck in image-based automated plant phenotyping. We classify approaches to the analysis of automated image-based plant phenotyping into two broad categories, namely, holistic and component-based. Holistic analyses consider the whole plant as a single object and measure its attributes, whereas component-based phenotyping analyzes the individual parts of a plant, i.e., individual leaves and stems. Two new holistic phenotypes are introduced in this paper, i.e., bi-angular convex-hull area ratio and plant aspect ratio. Bi-angular convex-hull area ratio is defined as the ratio of the area of the convex-hull of the plant when viewed from the side at a particular angle and the convex-hull of the same plant when viewed at a rotation of 90°. Changes in bi-angular convex-hull area ratio provide information about temporal change in phyllotaxy, i.e., the arrangement of leaves around a stem. Plant aspect ratio is defined as the ratio of the height of the bounding rectangle of the plant viewed from the side and the diameter of the minimum enclosing circle of the plant when viewed from directly above. Plant aspect ratio identifies potential differences in the canopy architecture which would be generated by different crop accessions in the field. Two component-based phenotyping parameters are also computed: number of leaves, and the length of each leaf. The paper introduces a benchmark dataset called Panicoid Phenomap-1, which comprises images of 40 genotypes of panicoid grain crops

captured by visible light camera once daily for 26 days using the Lemnatec scanalyzer 3D high throughput plant phenotyping facility at the University of Nebraska-Lincoln, USA, to facilitate vegetative-stage temporal phenotyping analysis. Experiments are performed on Panicoid Phenomap-1 dataset to demonstrate the genetic regulation of variation in these phenotypes in maize.

Keywords

Plant phenotyping, vegetative stage, panicoid grain crops, maize plants, contour extraction, skeletonization.

1. INTRODUCTION

Image based plant phenotyping has the following desirable characteristics relative to many other methods of collecting plant phenotypic data: 1) non-invasive, i.e., phenotypic traits can be measured without damaging the plants being measured; 2) tractable to automation, i.e., with properly engineered systems, very little, or no manual intervention or physical human labor is required; 3) scalable, i.e., large population of plants can be analyzed in short period of time.

For image-based plant phenotyping to provide meaningful results, it is necessary to extract numerical phenotypes from images of the plants. These numerical phenotypes enable statistical analysis of phenotypic variation, correlation across different traits, and the mapping of genetic loci which regulate variation in target phenotypes. Image-based plant phenotyping is often applied in a high throughput fashion to monitor and quantify changes in the parameters of phenotypic traits for individual plants at regular intervals under various environmental conditions.

The panicoid grasses are a group of species which share similar plant architectures and include a number of important food and biofuel crops, e.g., maize, sorghum, sugar cane, foxtail millet, proso millet, Miscanthus, and switchgrass. Among these crops, maize (*Zea mays ssp mays*), also called corn, is the most widely studied by plant biologists, and is one of the three grain crops responsible for directly or indirectly providing half of the world's total calorie con-

^{*}Corresponding author.

Permission to make digital or hard copies of all or part of this work for personal or classroom use is granted without fee provided that copies are not made or distributed for profit or commercial advantage and that copies bear this notice and the full citation on the first page. Copyrights for components of this work owned by others than ACM must be honored. Abstracting with credit is permitted. To copy otherwise, or republish, to post on servers or to redistribute to lists, requires prior specific permission and/or a fee. Request permissions from permissions@acm.org.

DS-FEW '16 August 14, 2016, San Francisco, CA, USA

© 2016 ACM. ISBN 123-4567-24-567/08/06...\$15.00

DOI: 10.475/123.4

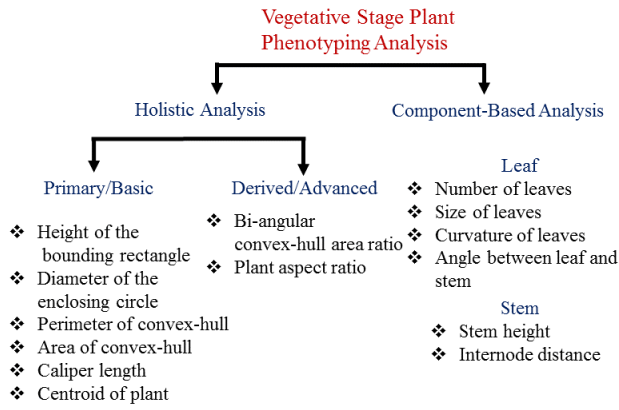


Figure 1: Classification of vegetative stage plant phenotyping analysis.

sumption.

Recent image-based nondestructive approaches to plant phenotyping in controlled environments have mainly considered *Arabidopsis* (*Arabidopsis thaliana*) and tobacco (*Nicotiana tabacum*) as the model plants for the study of leaf segmentation using 3-dimensional histogram cubes and superpixels [11], plant growth and chlorophyll fluorescence analysis in relation to abiotic stress situations using imaging technique called GROWSCREEN FLUORO[6], and automated plant segmentation using active contour model [10]. Being motivated by the lack of study of automated plant phenotyping analysis in the case of maize plants, we develop fully automated software systems to compute new phenotypes over a significant time interval of the vegetative stage life cycle of maize plants, and provide detailed experimental analysis to study the effect of these temporal phenotypes on intraspecies genetic variation on our benchmark dataset.

The paper has the following novelties: (a) it introduces the benchmark dataset called Panicoid Phenomap-1 to facilitate the development of new algorithms for extracting meaningful phenotyping parameters from images of panicoid grain crops; (b) it introduces fully automated software systems to compute new phenotypes with a discussion on their significance in the field plant science; (c) it provides an algorithm for leaf-count and leaf-size measurement; and (d) analyses are performed on the maize accessions included in the Panicoid Phenomap-1 dataset to determine the degree to which these phenotypes are regulated by genetic variation.

The paper is organized as follows. Section 2 describes phenotyping parameters computable by computer vision techniques under two broad categories: holistic and component-based, and Section 3 provides the methodology to compute these phenotyping parameters. Section 4 introduces the Panicoid Phenomap-1 dataset and Section 5 provides experimental results. Finally, Section 6 concludes the paper.

2. PHENOTYPES

We classify plant phenotypes into two categories: (a) holistic and (b) component-based. Holistic analysis considers the whole plant as a single object to quantify its geometrical shape, whereas component-based phenotyping analyzes the individual parts of a plant, i.e., leaves and stems. Holistic phenotypes are classified as primary or basic, and derived or advanced. Primary holistic phenotyping analysis measures

the individual attributes of the basic geometrical shape, e.g., height of the bounding rectangle of a plant to quantify plant height, area of the convex-hull to quantify plant size. Derived holistic parameters combine two or more primary phenotypes for advanced plant phenotyping analysis. Fig. 1 shows the classification of vegetative stage plant phenotyping analysis.

Leaves are one of the primary organs of plants which transform solar light energy into chemical energy in the form of sugars through photosynthesis. Total leaf area is associated with photosynthetic rate [3]. Maize plants have been shown to alter leaf positioning (i.e., phyllotaxy) in response to light signals perceived through the photochrome pathway in order to optimize light interception [9]. Automated phenotyping analysis using images of individual plants captured once per day from multiple angles made it possible for us to study how different maize inbreds altered their phyllotaxy at different points in development. We introduce a new derived holistic phenotype, namely, bi-angular convex-hull area ratio ($BACHR$), which is defined as

$$BACHR = \frac{Area_{CH} \text{ at side view } 0^\circ}{Area_{CH} \text{ at side view } 90^\circ}, \quad (1)$$

where, $Area_{CH}$ is the area of the convex-hull.

Variation in canopy architecture influences the proportion of incident solar radiation which can be intercepted by leaves, and thus it also influences the proportion of this energy which can be converted to chemical energy. Increases in field planting density over the last century have shifted the ideal ideotype for maize plants towards more erect leaf angles. Leaf erectness has traditionally been measured by quantifying the angle between a specifically defined leaf and the stem of the plant. High planting densities also trigger the shade avoidance response, triggering plants to invest more energy in stem elongation at the expense of yield. Artificial selection for yield at high planting densities [1] has also driven a reduction in the shade avoidance response of maize hybrids, likely also mediated through the phytochrome pathway [2]. Here we sought to develop and test an alternative derived holistic phenotype which we call as plant aspect ratio (PAR) that integrates data on plant height and leaf extent.

PAR is defined as

$$PAR = \frac{Height_{BR} \text{ at side view}}{Diameter_{MEC} \text{ at top view}}, \quad (2)$$

where, $Height_{BR}$ and $Diameter_{MEC}$ respectively denote the height of the bounding rectangle (BR) of the plant in side view 0° , and the diameter of the minimum enclosing circle (MEC) of the plant in top view. Plant aspect ratio is a metric for distinguishing between genotypes with narrow versus wide leaf extent after controlling for plant height. The height of the bounding box enclosing a plant from the side view is not affected by the angle of leaves relative to the camera, however, the angle of leaves relative to the camera does influence the apparent width of the plant as viewed from the side. Hence, to compute plant aspect ratio, we consider the height of the plant from the side view and the diameter of the minimum enclosing circle of the plant from the top view, as the diameter of the minimum enclosing circle in the top view provides a good approximation of the actual width of the plant while being unaffected by the angle of plant leaves relative to the camera. Since, bi-angular convex-hull area ratio and plant aspect ratio are the ratios

of two parameters of same units, they are independent of change in scale.

Plants are not static, but changing organisms with consistently increasing complexity in shape and appearance over time [11]. The growth of a plant is best interpreted by the number of leaves and the size of each leaf. Thus, for component-based phenotypes, we introduce an algorithm to count the number of leaves of a plant, and measure the size of each leaf.

3. METHODOLOGY

3.1 Background subtraction

To compute temporal phenotyping parameters, it is necessary to analyze a sequence of images captured daily for each plant as it grows over time. The first step is to segment the growing plant (foreground) from the background, i.e., the part of the scene which remains static over the period of interest, for the image sequences. The foreground, i.e., the plant, is segmented based on simplest frame differencing technique of background subtraction [4]. The grayscale foreground image thus obtained, is binarized using 2D Otsu automatic thresholding technique [7], which utilizes both the grey level information of each pixel and its spatial correlation information within the 2D neighborhood. The binary image is subjected to connected-component analysis involving morphological operation of dilation to remove noisy pixels and followed by erosion to fill up any small holes inside the plant image to give a single connected region.

3.2 Plant contour extraction

The speed of execution is increased if the computer vision operations are allowed to process a region of interest. Since the imaging chambers of Lemnatec scanalyzer 3D high throughput plant phenotyping system has a fixed homogeneous background, we use physical measurements to set the region of interest as the region that could be occupied by the maximally grown corn plant. Within the region of interest, the contour of a plant is extracted as the sequence of vertices using a traversal algorithm based on connectivity [4].

The process of contour extraction often results in a few small contours due to segmentation noises in the region of interest in addition to the desired plant contour of the largest size. The perimeters of the extracted contours are computed to keep the contour with largest perimeter as the desired plant, while reducing the perimeters of all smaller contours to zero to get rid of noises. Fig. 2(a)-(e) show the original images of a maize plant captured from side view 0° on different days and Fig. 2(f)-(j) show the corresponding contours enclosed by the convex-hull. Similarly, Fig. 2(k)-(o) show the original images of a maize plant captured from side view 90° on different days and Fig. 2(p)-(t) show the corresponding contours enclosed by the convex-hull. Fig. 4(f)-(j) show the contours enclosed by the bounding rectangle of the original plant images from side view 0° as shown in Fig. 4(a)-(e), respectively, and Fig. 4(p)-(t) show the contour enclosed by the minimum bounding circle of the original plant images from top view as shown in Fig. 4(k)-(o), respectively.

3.3 Skeletonization

To compute the component-based parameters, i.e., (a) number of leaves, (b) size of each leaf, the binary plant is

reduced to one-pixel wide lines using a parallel thinning algorithms based on iterative deletion of pixels in two sub-iteration steps as explained in [5]. The most important step after image thinning is to find the co-ordinates of the junction points (leaf-nodes) and the co-ordinates of the tip of the leaves. To detect each leaf, we start at the tip of the leaves and traverse the image pixels until we encounter the junction points. The image pixels thus traversed in succession, is the leaf edge. Fig. 3 (a) and (c) show the original images of two maize plants, and Fig. 3 (b) and (d) show the leaves marked with random colors of the plants in (a) and (c), respectively. The size of each leaf as mentioned in the figure, is measured in terms of number of pixels along the skeleton from the leaf-tip to the junction point. The algorithm to detect and count the total number of leaves and measure the size of each leaf is provided in Algorithm 1.

Algorithm 1 Computation of the number of leaves and the size of each leaf of a plant

Input: The original side view images of the maize plants from Panicoid Phenomap-1 dataset.

Output: Plant images with all leaves marked with random colors and each leaf is associated with size in terms of pixel units.

- 1: The foreground, i.e., the plant, is extracted from the original image using frame differencing technique of background subtraction followed by removal of non-green pixels.
 - 2: Binarize the extracted foreground using Otsu's thresholding technique.
 - 3: Skeletonize the binary image.
 - 4: Determine the co-ordinates of the end points (leaf-tip) and the junctions (leaf-node) of the skeleton image by using Peter Kovese's edge linking and line segment fitting functions in Matlab from [8].
 - 5: Traverse along the skeleton starting from the leaf-tip until it meets at the junction. The part of skeleton enclosed between leaf-tip and leaf-junction is marked as a leaf.
 - 6: Display the size of each leaf in terms of number of pixels between the leaf-tip and leaf-junction along the skeleton.
-

4. PANICOID PHENOMAP-1 DATASET

4.1 Capturing system

Fig. 5 shows the Lemnatec scanalyzer 3D high throughput plant phenotyping system at the University of Nebraska-Lincoln, USA, which is used to capture multi-sensor phenotyping measurements of plants in a non-destructive fashion on a daily basis. Our conveyor system has the capacity to host 672 plants with heights up to 2.35 meters. It has three watering stations with balance can add water to target weight or specific volume and records the specific quantity of water added on a daily basis.

Each plant is placed in a carrier upon the conveyor belt which moves the plants from the greenhouse to the four imaging cabinets in succession for capturing images. The cameras fitted in the four imaging cabinets from left to right are (a) visible light side view and top view, (b) infrared side view and top view, (c) fluorescent side view and top view, and (d) hyperspectral side view and near infrared top view. The images are captured using five different imaging modal-

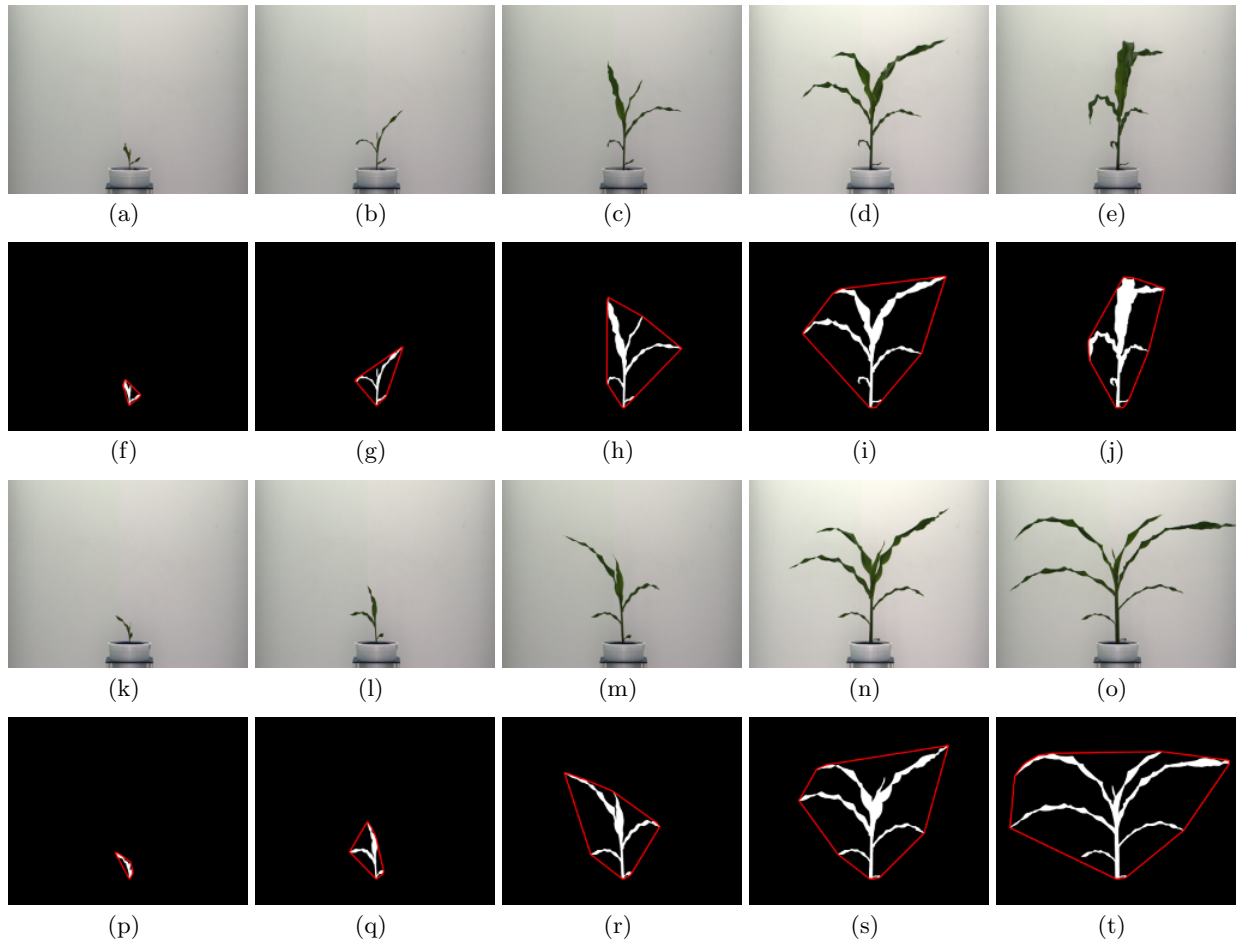


Figure 2: Computation of bi-angular convex-hull area ratio: rows 1 and 3- Original images of a maize plant at side view 0° and 90° , respectively on (a) and (k) Day 6, (b) and (l) Day 10, (c) and (m) Day 16, (d) and (n) Day 22, and (e) and (o) Day 24. Rows 2 and 4-contours enclosed by the convex-hull of the corresponding images in rows 1 and 3, respectively.

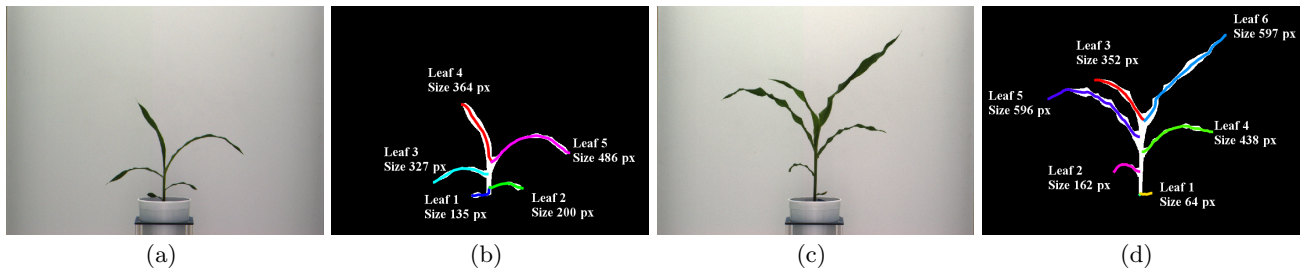


Figure 3: Illustration of component-based phenotyping analysis for leaf-count and leaf-size measurement: (a) and (c) Original images of maize plants captured on two different days; (b) and (d) Plants with leaves marked with random colors and each leaf is associated with its size measured in pixel units of images in (a) and (c).

Table 1: Specifications of different types of cameras of the Lemnatec scanalyzer 3D high throughput plant phenotyping system at the University of Nebraska-Lincoln, USA.

Camera Type	Spatial Resolution(px)	Spectral range (nm)	Band	frame rate (fps)	Bit Depth (bit)
Visible light	2454 x 2056	400-700	-	17	24
Fluorescent	1390 x 1038	620-900	-	24	14
Infrared	640 x 480	8-14	-	5	14
Near-infrared	640 x 480	900-1700	-	24	14
hyperspectral	320 line width	545-1700	243	100	16

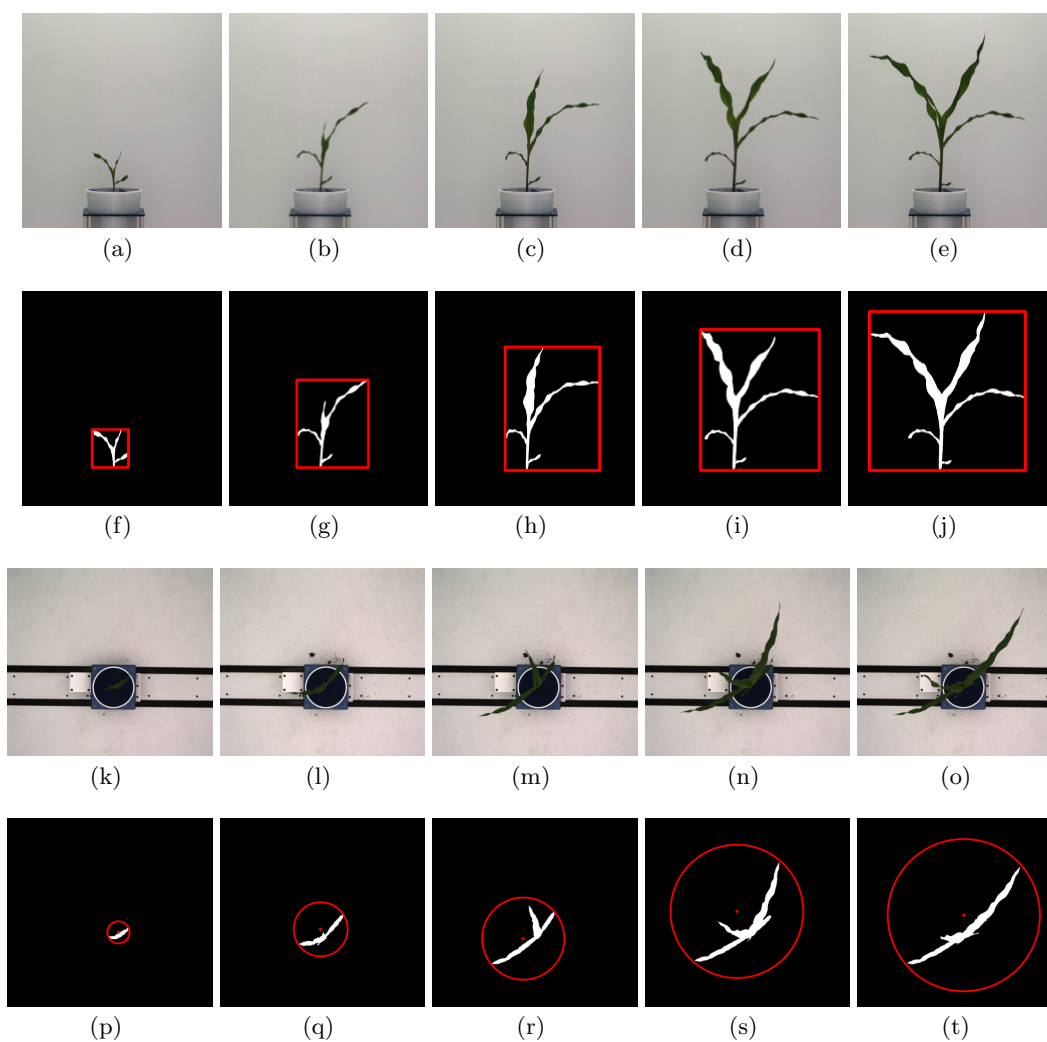


Figure 4: Computation of plant aspect ratio: rows 1 and 3- Original images of a maize plant at side view 0° and top view on (a) and (k) Day 7, (b) and (l) Day 11, (c) and (m) Day 14, (d) and (n) Day 17, (e) and (o) Day 18. Rows 2 and 4- contours enclosed by the bounding rectangle and minimum enclosing circle of the images in rows 1 and 3, respectively.



Figure 5: Lemnatec scanalyzer 3D system at the University of Nebraska-Lincoln, USA, for high throughput plant phenotyping: (a) view of the greenhouse; (b) Lemnatec imaging chambers; (c) plant entering into the visible light chamber; and (d) plant entering into the fluorescent chamber.

ities: visible light, fluorescent, infrared, near infrared and hyperspectral. Each imaging cabinet has rotating lifters for up to 360 side view images. Table 1 shows the specifications of all types of cameras.

4.2 Dataset organization

This paper introduces Panicoid Phenomap-1 which contains images of 40 total genotypes including at least one representative accession from five panicoid grain crops: maize, sorghum, pearl millet, proso millet and foxtail millet. Images were collected once per day for 26 days. The imaging started two days after planting the seeds. The dataset is designed to facilitate the development of new computer vision algorithms for the extraction of holistic phenotypic parameters specifically from maize and to encourage researchers to test the effectiveness of these algorithms to related crop species with similar plant architectures. This dataset is also an ideal candidate for evaluating leaf segmentation, leaf alignment and leaf tracking algorithms, as well as computation of a diverse set of component-based phenotypes.

The folder for each plant is named as Plant ID-genotype ID. Table 2 shows the names of the genotypes corresponding to the genotype IDs used in the dataset. Each folder is subdivided into three subfolders, namely, SideView0, SideView90 and TopView. SideView0 contains 26 images (named as Day_001.png, Day_002.png, ..., Day_026.png) captured from 0° angle, SideView90 contains 26 images captured from 90° angle and top view contains 26 images captured from the camera located at the top of the chamber. Thus, each folder contains $26 \times 3 = 78$ images for 3 views (side view 0°, side view 90° and top view), totalling $78 \times 176 = 13728$ images, where 176 are the total number of plants. To be consistent with the capturing side view angles, all seeds were planted in the pots placed on the conveyor belt with the same orientation as determined by the embryo (concave area on the side of the seed) pointing towards the north side of the greenhouse. The plants were never rotated while they were on the belt, and thus, side view 0° in the dataset implies that the line of sight of the camera is perpendicular to the axis of the germ of the kernel. Each chamber has a pneumatic lifter with an electric motor rotator that rotates the plant to the required angle, i.e., 90°, to capture side view 90° images included in the dataset. The dataset is freely available from <http://plantvision.unl.edu>.

5. EXPERIMENTAL ANALYSIS

5.1 Experimental setup

Images captured from dated October 11, 2015 to November 04, 2015 (referred to as Day_002 to Day_026 in Panicoid Phenomap-1), were analyzed. The greatest difference in plant phyllotaxy angle was computed for data from day seven onward, as prior to day seven, several individual plants were too small to yield consistent results. Plant aspect ratio was quantified on Day 15 and Day 25. Several plants with aspect ratios greater than 2.5 were only removed from the visualization in order to increase readability. One genotype (PHG35, genotype ID 22) exhibited poor germination (20%) and was removed through the analysis. Purple Majesty, genotype ID 36, did not germinate at all.

5.2 Discussion

Table 2: The genotype names corresponding to the genotype IDs used in the dataset. Keys- G_{ID} : genotype ID and G_{name} : genotype name.

G_{ID}	G_{name}	G_{ID}	G_{name}
1	740	21	DHB47
2	2369	22	PHG35
3	A619	23	PHG39
4	A632	24	PHG47
5	A634	25	PHG83
6	B14	26	PHJ40
7	B37	27	PHH82
8	B73	28	PHV63
9	C103	29	PHW52
10	CM105	30	PHZ51
11	LH123HT	31	W117HT
12	LH145	32	Wf9
13	LH162	33	Yugu1
14	LH195	34	PI614815
15	LH198	35	PI583800
16	LH74	36	Purple Majesty
17	LH82	37	BTx623
18	Mo17	38	PI535796
19	DKPB80	39	PI463255
20	PH207	40	PI578074

The boxplots in Fig. 6(a) and (b) respectively show the results of analysis for the bi-angular convex-hull area ratio and plant aspect ratio using the experimental setup described above. The boxplots were generated using matplotlib. Heritability of all three values were estimated through ANOVA as described in [12]. Since plant aspect ratios for Day 15 and Day 25 showed skewed distributions of values, spearman correlation between median values of aspect ratios of Day 15 and 25 for each genotype were calculated.

The median value of bi-angular convex-hull area ratio for all selected corn lines was within 0.5-5. Specifically, the highest value 4.54 appeared in the corn line PHV63 while the common reference genotype B73 was in the middle of the range with the value 1.56. The estimated heritability - the proportion of total variation which can be explained by genetic variation- for bi-angular convex-hull area ratio was calculated to be 24.85%. This moderate value suggests that the observed rotation is only partial under the direct control of genetics and is likely also regulated by environment factors as well as genotype by environment interactions. We hypothesize that edge plants were exposed to significantly different red-far red ratios that plants in the center of our experimental layout, resulting in different signals being passed through the phytochrome signalling pathway. In addition to this type of micro-environment variation, the non-heritable portion of variance will also include any inaccuracy in quantification created by the software itself.

We also visualized variation in aspect ratio within the same accessions between Day 15 and Day 25, with accessions sorted by ascending order based upon Day 15 values. In general, most genotypes exhibited higher plant aspect ratio values on Day 15 than on Day 25. Heritability for plant aspect ratio was also significantly higher on Day 15 (23.23%) than on Day 25 (14.00%). Plant aspect ratio is a derived trait calculated from the combination of plant height and diameter, which are 67.7% and 37.6% for Day 15 as well as 67.1% and 51.2% for Day 25 respectively. We hypothesize that the

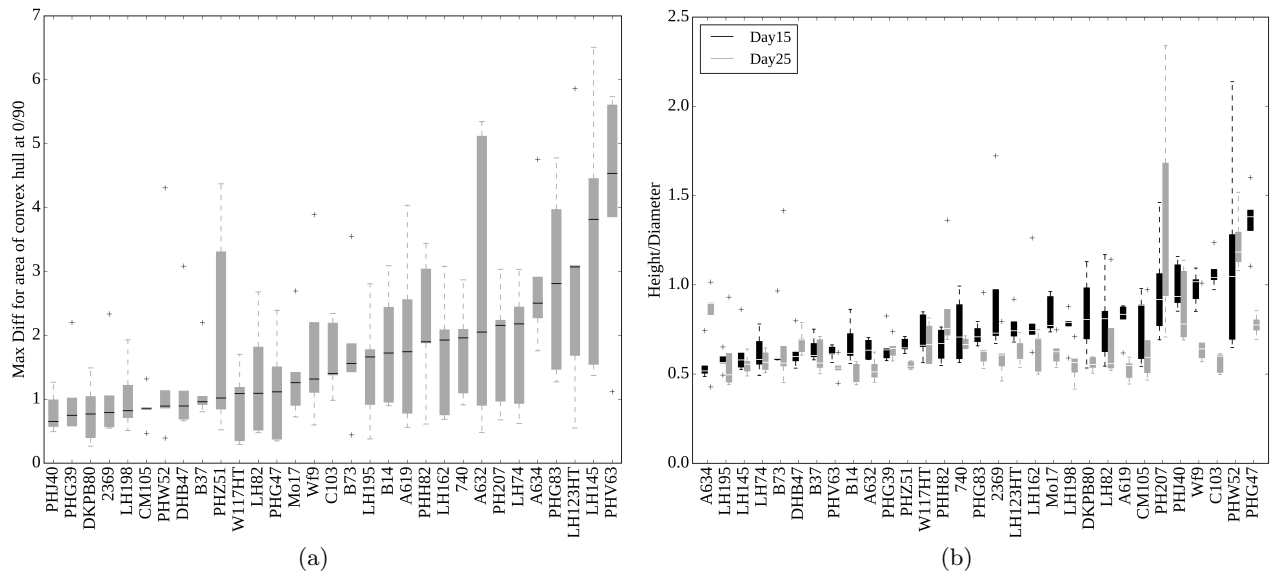


Figure 6: Results of experimental analysis using boxplots for (a) bi-angular convex-hull area ratio ($BACHR$); and (b) plant aspect ratio (PAR).

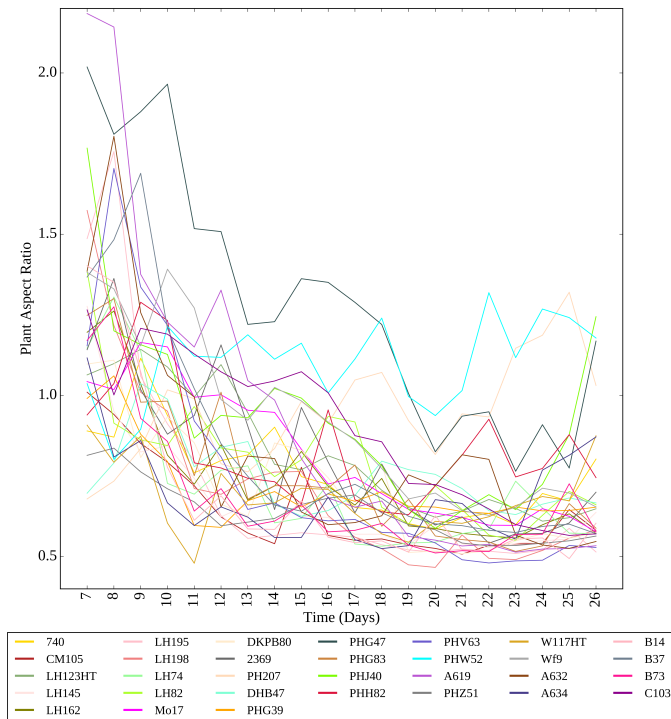


Figure 7: Illustration of genetic regulation of plant aspect ratio (PAR).

greatly reduced heritability of the plant aspect ratio relative to its component elements on Day 25 is because each of these traits is correlated with absolute plant size which was also highly heritable. The genotype with the highest aspect ratio in Day 15 datasets was PHG47, and the second highest was PHW52. PHW52 had extremely high plant-to-plant variation in aspect ratio. Interestingly, PHW52 was the genotype with the largest aspect ratio in Day 25. The genotype with the largest plant to plant variation such as PH207 in Day 25 and PHW52 in Day 15 contributed much to both genetic and residual variation. Plant aspect ratio showed a moderately statistically significant positive correlation between Day 15 and Day 25 ($r=0.356$, $P\text{-value}=0.049$). Therefore, Day 15 aspect ratios of corn lines can only explain 13.3% of the variation in Day 25 aspect ratios. This suggests that studies of maize adult plant architecture require phenotyping plants at more mature stages of development as early developmental stage measurements have only moderate predictive value at later stages in development.

Fig. 7 shows the average plant aspect ratio for all plants of each of 31 genotypes through Day 7 to Day 26. It is evident from the figure that the plant aspect ratio for several genotypes, e.g., 2369 and C103, decreases significantly with time, which supports the fact that the rate of increase in plant width is more compared to the plant height. However, plant aspect ratios for genotypes PHW52 and PHG39 fluctuate between two fairly similar values for Day 7 (1.04 and 0.99 for PHW52 and PHG39 respectively) and Day 26 (1.18 and 0.65 for PHW52 and PHG39 respectively). It is also to be noted that some genotypes have higher plant aspect ratios (e.g., PHG47) compared to the others (e.g., B73). These inferences clearly demonstrate the potential of plant aspect ratio to be an effective phenotype regulated by genetic variation.

5.3 Software description and runtime complexity analysis

Two fully automated software systems, i.e., software A and software B are developed to respectively compute two holistic phenotypes introduced in the paper, i.e., (a) bi-angular convex-hull area ratio and (b) plant aspect ratio, using OpenCV [4] and C++ on Visual Studio 2010 Express Edition. Software A accepts the original images of the Panicoid Phenomap-1 dataset as input, and results in the three text files, i.e., ratio.txt to contain the values for bi-angular convex-hull area ratio for all images, sideview0.txt to contain the area of convex-hull of the side view 0° images, and sideview90.txt to contain the area of the convex-hull of the side view 90° images.

Similarly, software B accepts the original images of Panicoid Phenomap-1 dataset as input, and results in the three text files, i.e., sideview.txt to contain the values for the height of the bounding rectangle of all side view images, topview.txt to contain the values for diameter of the minimum enclosing circle for all top view images, and ratio.txt to contain the plant aspect ratio for all images. Software A automatically creates two folders called sideview0 and sideview90 to respectively save the end images as shown in Fig. 2(f)-(j) and Fig. 2(p)-(t) during execution. Similarly, software B also automatically creates two folders called sideview and topview to save the end images as shown in Fig. 4(f)-(j) and Fig. 4(p)-(t), respectively, during execution. The execution time for software A and software B on an Intel(R)Core(TM) i7 processor with 16 GB RAM working at 2.60-GHz using 64 bit Windows 7 operating system are respectively 2.15 hours and 2.23 hours measured using CPU clock time for Panicoid Phenomap-1 dataset.

6. CONCLUSIONS

The paper introduces Panicoid Phenomap-1 dataset to facilitate vegetative stage phenotyping analysis of panicoid grain crops using visible light images. The images are captured using Lemnatec scanalyzer 3D high-throughput plant phenotyping facility at the UNL, USA. Two automated software packages have been developed to compute two new advanced holistic phenotypes, namely, bi-angular convex-hull area ratio and plant aspect ratio. Experimental analyses are performed on Panicoid Phenomap-1 to demonstrate the effectiveness of bi-angular convex-hull area ratio and plant aspect ratio to respectively explain phyllotaxy and canopy architecture of different genotypes of maize plants.

The paper introduces an algorithm to compute component-based phenotypes, i.e., total number of leaves and size of each leaf of a plant. The main challenge in quantifying component-based phenotypes based on imaging techniques is self-occlusions. Thus, our future work will consider to develop advanced algorithms to compute component-based phenotypes by considering multiple views of the plants to address self-occlusions. The future work will also consider to release a larger dataset comprising multimodal image sequences of higher numbers of diverse panicoid crop varieties.

7. ACKNOWLEDGMENTS

The authors would like to thank the Agricultural Research Division in the Institute of Agriculture and Natural Resources of the University of Nebraska-Lincoln, USA, for providing the funds for this research.

8. REFERENCES

- [1] B. Brekke, J. Edwards, and A. Knappa. Selection and adaptation to high plant density in the Iowa stiff stalk synthetic maize (*Zea mays* L.) population: II. plant morphology. *American Society of Agronomy*, 51:2344–2351, 2011.
- [2] P. Dubois, G. Olsefski, S. Flint-Garcia, T. Setter, O. Hoekenga, and T. Brutnell. Physiological and genetic characterization of end-of-day far-red light response in maize seedlings. *Plant Physiology*, 154:173–186, 2010.
- [3] W. G. Duncan. Leaf angles, leaf area, and canopy photosynthesis. *Crop Science*, 11(4):482–485, 1971.
- [4] G. B. Garcia, O. D. Suarez, J. L. E. Aranda, J. S. Tercero, and I. S. Gracia. *Learning Image Processing with OpenCV*. Packt Publishing Ltd, Birmingham, UK, 2015.
- [5] Z. Guo and R. W. Hall. Parallel thinning with two subiteration algorithms. *Communications of the ACM*, 32(3):359–373, 1989.
- [6] M. Jansen, F. Gilmer, B. Biskup, K. A. Nagel, U. Rascher, A. Fischbach, S. Briem, G. Dreissen, S. Tittmann, S. Braun, I. D. Jaeger, M. Metzloff, U. Schurr, H. Scharr, and A. Walter. Simultaneous phenotyping of leaf growth and chlorophyll fluorescence via growSCREEN fluoro allows detection of stress tolerance in *Arabidopsis thaliana* and other rosette plants. *Functional Plant Biology*, 36.
- [7] L. Jianzhuang, L. Wenqing, and T. Yupeng. Automatic thresholding of gray-level pictures using two-dimension otsu method. In *International Conference on Circuits and Systems*, pages 84–89. China, March 1991.
- [8] P. D. Kovese. MATLAB and Octave functions for computer vision and image processing, 2000. Available from: <<http://www.peterkovese.com/matlabfns/>>.
- [9] G. A. Maddonni, M. E. Otegui, B. Andrieu, M. Chelle, and J. J. Casal. Maize leaves turn away from neighbors. *Plant Physiology*, 130(3):1181–1189, 2002.
- [10] M. Minervini, M. M. Abdelsamea, and S. A. Tsafaris. Image-based plant phenotyping with incremental learning and active contours. *Ecological Informatics*, 23:35–48, 2014.
- [11] H. Scharr, M. Minervini, A. P. French, C. Klukas, D. M. Kramer, X. Liu, I. Luengo, J. Pape, G. Polder, D. Vukadinovic, X. Yin, and S. A. Tsafaris. Leaf segmentation in plant phenotyping: a collation study. *Machine Vision and Applications*, 27(4):585–606, May 2016.
- [12] A. M. Thompson, J. Yu, M. C. Timmermans, P. Schnable, J. C. Crants, M. J. Scanlon, and G. J. Muehlbauer. Diversity of maize shoot apical meristem architecture and its relationship to plant morphology. *G3: Genes| Genomes| Genetics*, 5(5):819–827, 2015.